WPPMI-PR(18) 19532

R Ambrosino et al.

Optimization of the PF coil system in axisymmetric fusion devices

Preprint of Paper to be submitted for publication in
Fusion Engineering and Design

This work has been carried out within the framework of the EUROfusion Consortium and has received funding from the Euratom research and training programme 2014-2018 under grant agreement No 633053. The views and opinions expressed herein do not necessarily reflect those of the European Commission.

Optimization of the PF coil system in axisymmetric fusion devices

R. Albanese, R. Ambrosino, A. Castaldo, V.P. Loschiavo

Consorzio CREATE and DIETI - Università degli Studi di Napoli Federico II, Via Claudio 21, I-80125 Napoli, Italy
{raffaele.albanese, roberto.ambrosino, antonio.castaldo, vincenzopaolo.loschiavo}@unina.it

Abstract

Tokamak is nowadays the most promising fusion device for the plasma confinement and the production of fusion energy. It exploits powerful magnetic fields to confine plasma inside a torus shaped chamber. The magnet system of a tokamak device is mainly composed by Toroidal Field (TF), Central Solenoid (CS) and Poloidal Field (PF) coils. In this paper, a new approach is described for the optimization of the PF coil system. The proposed procedure allows to optimize the number, position and dimension of the PF coils reducing, at the same time, currents and forces on the coils while fulfilling the machine technological constraints. The method exploits the linearized relation between the plasma-wall gaps and the PF coil currents. The procedure effectiveness has been tested and exploited for the design and optimization of the PF coil system for the next generation tokamak DEMO, as shown in the last section of the paper.

Keywords: *tokamak, plasma fusion, optimization problem*

1 Introduction

Nuclear fusion is one of the most promising way of obtaining energy supply in a clean and in principle inexhaustible way. The most advanced devices for hot nuclear fusion are tokamaks, toroidal axisymmetric structures where the plasma is magnetically confined due to the interaction with magnetic fields produced by the currents flowing in suitable coils placed around the chamber. The main project in this field is ITER [1], an experimental reactor that is under construction in France. At the same time, the pre-conceptual design phase towards the realization of DEMO [2]-[3], the first reactor producing net electricity for the grid, is already started.

The magnet system of a tokamak device is mainly composed by Toroidal Field (TF), Central Solenoid (CS) and Poloidal Field (PF) coils. The CS is sometimes referred to as primary transformer (see Figure 1). To minimize the Joule losses in the coil windings, all magnets of future generation tokamaks will be made of superconducting wires. The TF coils set produces a magnetic field strength within the toroidal volume bounded by its coils. The CS and PF coils sets generate a magnetic field that, on the contrary, permeates the whole space and it is designed to shape the plasma and to drive inductively its current.

The design of the CS/PF coil system is a complex problem due to the nonlinear relation between the plasma shape variation and the currents in the CS/PF coils. Moreover, a set of linear and nonlinear technological constraints related to the maximum current density, magnetic fields and vertical forces on the coils has to be satisfied. The previous considerations make the optimization of the number, position and dimension of the PF coils a challenging task in the design of the next generation fusion reactors.

In this paper, an optimization procedure of the PF/CS coil system is proposed. Given a reference plasma scenario, the procedure is able to optimize PF coils number, position and dimension guarantying all the machine technological constraints. This approach is an extension of the procedure used for the optimization of the PF coil currents in existing devices [4]. It is based on the linearization of the Grad-Shafranov (GS) equation for the plasma magneto-hydrodynamic (MHD) equilibrium evaluation around the desired plasma equilibrium ([5]-[6]); then an iterative quadratic optimization problem with linear and quadratic constraints is solved. In previous studies (e.g., [4]), the PF coil system optimization problem was mainly formulated as a LQ minimization problem. Such a formulation allowed taking into account the linear constraints only. The novelty introduced in this paper is the formulation of the problem as a quadratic minimization problem that allows taking into account also quadratic constraints, mainly related to the vertical forces acting on the coils.

The proposed solution, which dramatically simplifies the nonlinear computations needed for tokamak design, is currently being exploited for the optimization of the PF coil system in next generation tokamaks such as DEMO and DTT [8].
The paper is organized as follows: Section 2 defines the problem highlighting the importance of the plasma linearized model; Section 3 describes the proposed optimization procedure illustrating the constraints; Section 4 shows the results of the optimization method application to a DEMO standard single null (SN) plasma configuration. Finally, some conclusions are drawn in Section 5.

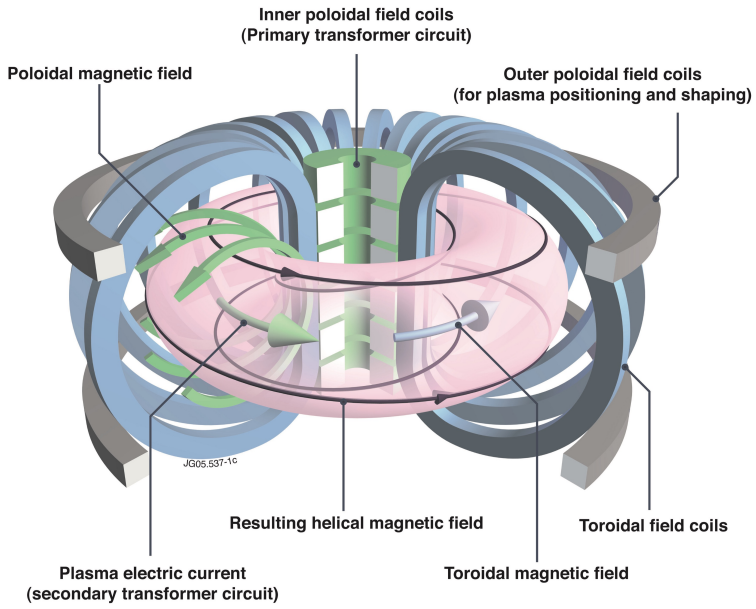

Figure 1. Schematic description of the toroidal and poloidal field coils (courtesy of EUROfusion)

2 Preliminaries

The definition and optimization of plasma configurations requires nonlinear equilibrium codes able to solve the Grad-Shafranov equation and linearized MHD equilibrium models describing the approximated plasma response to variations in the CS/PF coil currents. In this section, the description and a possible numerical solution of the GS equation is illustrated. The presented method is implemented in the equilibrium code CREATE-NL [9]. Then, a possible linearization of the GS equation is tackled. It can be performed numerically with a small variation method (e.g., by

approximating partial derivatives by finite differences, as in the CREATE-NL code), or analytically (e.g., by differentiating the Grad–Shafranov equation, as in the CREATE-L code [10].

2.1 2D axisymmetric nonlinear equilibrium model

Magneto-hydrodynamic (MHD) modeling is usually used to describe the plasma behavior in a tokamak. The system model is governed by plasma momentum balance and Maxwell's equations in their quasi-stationary form based on the following simplifying assumptions:

- the inertial term is disregarded on the slow time scale, hence the momentum balance becomes an evolutionary equilibrium equation;
- the tokamak plasma–circuit system is axisymmetric;
- to reproduce the interaction of the plasma with the active coils and the surrounding passive structures, the current density profile can be modeled with a finite number of global parameters, such as total plasma current I_p, poloidal beta β_p (related to the ratio between kinetic and magnetic pressure), and internal inductance l_i (a nondimensional quantity related to the magnetic energy stored inside the plasma) [11].

In axisymmetric geometry with cylindrical coordinates (r, φ, z), the MHD equilibrium of a two-dimensional plasma can be expressed in terms of two scalar functions, namely, the poloidal current function $f\ (r, z)$ and the poloidal magnetic flux per radian $\psi(r, z)$. The following set of partial differential equations (PDEs) can be used to describe a two-dimensional plasma equilibrium (illustrated in Figure 2):

$$\Delta^*\psi = -\mu_0 r j_{pl}(r, \psi, t) = -f\frac{df}{d\psi} - \mu_0 r^2 \frac{dp}{d\psi} \qquad \text{in plasma region} \qquad (1a)$$

$$\Delta^*\psi = -\mu_0 r j_{ext}(r, z, t) \qquad \text{in conductors} \qquad (1b)$$

$$\Delta^*\psi = 0 \qquad \text{elsewhere} \qquad (1c)$$

with the initial and boundary conditions:

$$\psi(r, z, t)|_{t=0} = \psi_0(r, z), \qquad \psi(r, z, t)|_{r=0} = 0 \qquad (2a)$$

$$\lim_{r^2+z^2\to\infty} \psi(r, z, t) = 0 \qquad (2b)$$

μ_0 is the magnetic permeability of the vacuum, j_{ext} is the toroidal current density in the external conductors (passive structures and active coils), $j_{pl}(r, \psi, t) = \frac{f}{\mu_0 r}\frac{df}{d\psi} + r\frac{dp}{d\psi}$, p is the kinetic pressure, Δ^* is the second-order differential operator:

$$\Delta^*\psi = r\frac{\partial}{\partial r}\left(\frac{1}{\mu_r r}\frac{\partial\psi}{\partial r}\right) + \frac{\partial}{\partial z}\left(\frac{1}{\mu_r}\frac{\partial\psi}{\partial z}\right) \quad . \qquad (3)$$

in which μ_r is the relative magnetic permeability.

The PDE (1a) describing the ψ map in the plasma region is known as the GS equation.

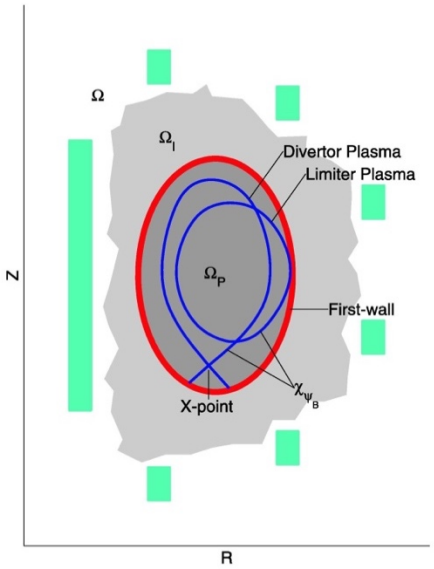

Figure 2. Poloidal view of an axisymmetric tokamak device. In green the conductors region and in dark grey the region accessible to the plasma.

PDEs (1a)–(1c) are used to calculate the poloidal flux ψ at time t, provided that the plasma boundary can be determined, the functions $p(\psi)$ and $f(\psi)$ are defined, and the toroidal current density in the PF coils is known. The plasma boundary is defined as the largest poloidal flux surface closed inside the vacuum vessel and is determined by a numerical calculation. Following [10], [11] and [11], we assume that, in the absence of edge currents, the functions $p(\psi)$ and $f\ (\psi)$ can be expressed in terms of three global parameters, namely plasma current I_p, poloidal beta β_p and internal inductance l_i; while the toroidal current density j_{ext} can be expressed as a linear combination of the PF circuit currents. Indeed, the plasma configuration and the magnetic flux can be determined when prescribing the vector of currents I (composed of plasma current and PF currents) along with the parameters β_p and l_i.
It is important to notice that, if we assume to directly impose the current density j_{ext} on the external circuits and the plasma current, the solution of (1a)–(1c) gives a static plasma equilibrium.

2.2. Equilibrium calculation with the finite element method

A free boundary equilibrium problem consists in finding the magnetic flux surfaces in the poloidal plane once the currents in the conductors are fixed, assuming a certain distribution of the plasma current. The solution of this problem also provides the boundary of the plasma, the largest poloidal flux surface closed inside the plasma region, as shown in Figure 2. The plasma boundary determines the region where the plasma is confined and it is fundamental for the definition of the plasma scenario and for the optimization of the CS/PF coils system. Indeed, in a free boundary equilibrium problem we assume that the PF currents, the plasma current I_p and the parameters β_p and l_i are fixed, while the flux map in the integration domain together with the plasma boundary are calculated as the solution of the set of PDEs in (1).
In order to recast the PDE equilibrium problem to a finite dimensional problem, a finite element method (FEM) can be used [9]. Indeed, the plasma current density can be approximated by means of a finite number of parameters using the following relationships:

$$j_{pl}(r,\psi,t) = \frac{f}{\mu_0 r}\frac{df}{d\psi} + r\frac{dp}{d\psi} \tag{4a}$$

$$p = p(\bar{\psi},\alpha) \qquad\qquad f = f(\bar{\psi},\alpha) \tag{4b}$$

$$\bar{\psi} = \frac{\psi - \psi_a}{\psi_b - \psi_a} \tag{4c}$$

where j_{pl} is the plasma current density, defined in terms the normalized flux $\bar{\psi}$ and of a set of suitable parameters α.
In the lumped parameter approach, the free boundary equilibrium problem requires the solution of a nonlinear set of equations:

$$F_{EQ}(\psi, I_{ext}, \alpha) = 0 \tag{5}$$

in which ψ is the vector of fluxes in the FEM spatial discretization nodes, I_{ext} is the set of external currents from which the spatial distribution of j_{ext} in (1b), and α, which the vector of parameters in (4b). Problem (5) can be solved with an iterative Newton-based method.

2.3. Plasma linearized model

Starting from the non-linear lumped parameters model, the following plasma linearized state space model [9]-[10] can easily be obtained:

$$\begin{aligned} \delta\dot{\boldsymbol{x}}(t) &= \boldsymbol{A}\delta\boldsymbol{x}(t) + \boldsymbol{B}\delta\boldsymbol{u}(t) + \boldsymbol{E}\delta\dot{\boldsymbol{w}}(t), \\ \delta\boldsymbol{y}(t) &= \boldsymbol{C}\delta\boldsymbol{x}(t) + \boldsymbol{F}\delta\boldsymbol{w}(t) \end{aligned} \tag{6}$$

where:

- $\boldsymbol{A}$, $\boldsymbol{B}$, $\boldsymbol{E}$, $\boldsymbol{C}$ and $\boldsymbol{F}$ are the model matrices;
- $\delta\boldsymbol{x}(t) = \left[\delta\boldsymbol{I}_{CS/PF}(t)\ \delta\boldsymbol{I}_e(t)\ \delta I_p(t)\right]^T$ is the state space vector;
- $\delta\boldsymbol{u}(t) = \left[\delta\boldsymbol{U}_{PF}(t)\ \boldsymbol{0}^T\ 0\right]^T$ are the input voltages variations;
- $\delta\boldsymbol{w}(t) = \left[\delta\beta_p(t)\ \delta l_i(t)\right]^T$ are the β_p and l_i variations;
- $\delta\boldsymbol{y}(t)$ are the output variations.

Among the outputs of the linearized model $\delta y(t)$, particular importance is assumed by the so called *gaps* δg, the measurements of the plasma–wall distances in different parts of the plasma region, as illustrated in Figure 3.

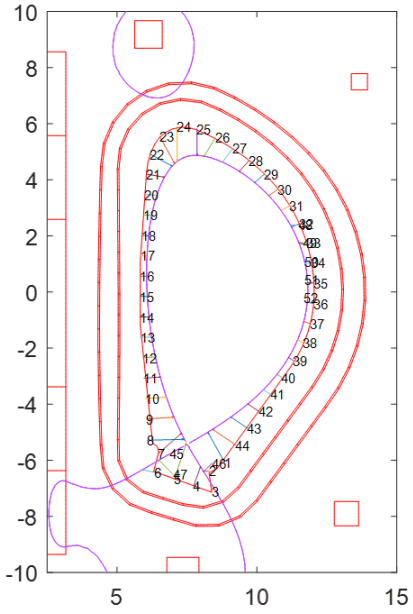

Figure 3. DEMO SN equilibrium with indication of the gaps.

Resorting to the linearized equations (6), small variations of the currents in the CS/PF coils ($\delta \boldsymbol{I}_{CS/PF}$) are related to small variations of the plasma shape ($\delta \boldsymbol{g}$) through a coefficient matrix ($\boldsymbol{C}_G$):

$$\delta \boldsymbol{g} = \boldsymbol{C}_G \delta \boldsymbol{I}_{CS/PF}. \tag{7}$$

Although the relation between the variation of the gaps and the PF currents is not linear, if the plasma boundary does not change too much, a linearization in (6)-(7) represents an important tool for the optimization of the PF coil system for a given set of plasma configurations.

3 Method description

The design of the PF coil system consists in the selection of an optimized number, position and cross-section of the PF coils suitable to produce a desired plasma scenario (plasma current profile and shape in different phases of a plasma shot). The design procedure is based on the solution of an optimization problem implemented on the linearized model of the plasma, as stated in equation (6). The optimized PF coils system has to guarantee a set of geometric constraints posed by the mechanical structures, the access specifications (e.g., ports, interference with the toroidal field (TF) coil system, etc.) and the plasma scenario operational constraints (e.g., bounds on the possible variations of the plasma parameters). In the following, the definition of the constraints will be firstly proposed; then, the optimization procedure will be described.

3.1 Constraints definition

In the following, a detailed description of the main constraints considered for the design of a tokamak PF coil systems is proposed.

PF coil currents

The cross-sections of the PF coils is determined by the maximum current density J_{max} $[A/m^2]$ in the coils. This limit is a gross value that takes into account the conductor jacket and the winding

packs. In the optimization procedure, the PF coil current limits turn out into linear constraints on the optimization variables $I_{CS/PF}$ in the form:

$$I^i_{CS/PF} \leq I^i_{max} \qquad i = 1 \dots N_{CS/PF}$$

where $N_{CS/PF}$ indicates the total number of PF and CS coils; I^i_{max} is the current limits in the i-th coil whose value depends on the current density limit J_{max} and the maximum area imposed for the coil.

Magnetic field

For a safe design of the conductors and the winding packs, a constraint on the maximum poloidal magnetic field B^{max}_{pol} at the location of the PF and CS coils needs to be imposed.

For an almost fixed plasma shape and current, the variation of the poloidal magnetic field in the CS/PF coil locations δB_{pol} during a plasma scenario depends linearly on the variation of the currents flowing in the coils $\delta I_{CS/PF}$, that is

$$\delta B_{pol} = \boldsymbol{C}_{B_{pol}} \delta I_{CS/PF}$$

where $\boldsymbol{C}_{B_{pol}} \in R^{N_{CS/PF} \times N_{CS/PF}}$ is part the output matrix in the linearized model in (6).
Concerning the CS stack, as matter of fact, the maximum operating magnetic field is found at the premagnetization, that is the initial instant of a plasma scenario when the CS modules carry the maximum current needed for the inductive plasma heating. Indeed, the width and position of the CS stack is usually done with an analytic premagnetization analysis able to guarantee the constraint of the maximum poloidal magnetic field [13].

Vertical Forces on the PF/CS coils

The independently fed PF/CS coils create large electromagnetic forces on the mechanical structures that pull in different directions. While the radial component of the electromagnetic force is balanced in axisymmetric tokamak, the vertical component needs to be bounded to lead the mechanical loads to acceptable values.
Vertical forces on the coils are proportional to the currents flowing in the coils and to the radial magnetic field in the coil location. Hence, for an almost fixed plasma shape and current, a quadratic dependence of the vertical forces on the PF/CS currents can be imposed. Vertical force constraints can be distinguished in:

- maximum vertical force on a single PF coil

$$\left|F^i_{PF}\right| \leq F^i_{PFmax} \qquad i = 1 \dots N_{PF} \tag{8}$$

  where N_{PF} indicates the number of PF coils and F^i_{PFmax} indicates the vertical force limit on the i-th PF coil;

- maximum vertical force on the CS stack

$$\left|\sum_{i=1}^{N_{CS}} F^i_{CS}\right| \leq F^{CS}_{max} \tag{9}$$

  where N_{CS} indicates the number of PF coils and F^{CS}_{max} indicates the vertical force limit on the CS;

- maximum separation force among the CS elements. Assuming the CS coils ordered from the top to the bottom, the separation force constraints are defined as

$$\sum_{i=1}^{k} F_{CS}^{i} \leq F_{sep\_up\_max}^{CS} \qquad i = 1 \dots N_{CS} \tag{10.1}$$

$$\sum_{i=1}^{k} F_{CS}^{N_{CS}-i+1} \geq -F_{sep\_down\_max}^{CS} \qquad i = 1 \dots N_{CS} \tag{10.2}$$

  where $F_{sep\_up\_max}^{CS}$ and $F_{sep\_down\_max}^{CS}$ indicate the absolute value of the vertical up and down separation force limits among the CS elements.

- *Plasma Separatrix*

Constraints on the plasma separatrix need to be imposed in order to ensure safe conditions for the plasma electromagnetic control and to reduce the power load on the plasma facing components. Indeed:

- to reduce the power load on the plasma facing components (PFCs) and to allow safe transient conditions in case of minor disruptions and L/H-H/L transitions, a minimum plasma-wall distance d_{min} needs to be guaranteed. Once the reference plasma shape is fixed, as stated in equation (7), a linear relation between the variation of the gaps δg and the variation of the currents $\delta I_{CS/PF}$ can be used to fulfill this constraint;
- to limit the power load on the divertor plate the grazing angle θ_g of the magnetic field at the strike points should be minimized [14]. However, for the divertor safe conditions, the minimum grazing angle in experimental fusion devices is around $1.5°$;
- to reduce the plasma growth rate and control the vertical unstable mode, the plasma elongation should not exceed a fixed limit;
- to maximize the fusion power performance, certain bounds are also imposed on the plasma triangularity [15] and on the minimum flux swing at flat-top [16].

3.2 Optimization procedure

In the following, it is assumed that the poloidal geometry of the device (first wall, divertor structure, vessel shells and TF coil shells) is already fixed. Moreover, the position and dimension of the CS stack has been already optimized in order to guarantee the poloidal magnetic field constraint at the premagnetization phase [13]. The proposed optimization procedure can be summarized as follows:

a) definition of a preliminary redundant PF coils system compatible with the available space, as shown in Figure 4;
b) design a reference plasma configuration at flat top (MHD equilibrium and linearized model) using the redundant PF coils system able to guarantee the plasma separatrix constraints on elongation, triangularity, plasma-wall gaps and grazing angle.
c) exhaustive analysis of all the candidate PF coil systems composed by a fixed number n of external PF coils chosen from the redundant system in order to find the PF configurations able to guarantee the currents and forces constraints while maintaining the desired plasma shape within a certain tolerance.

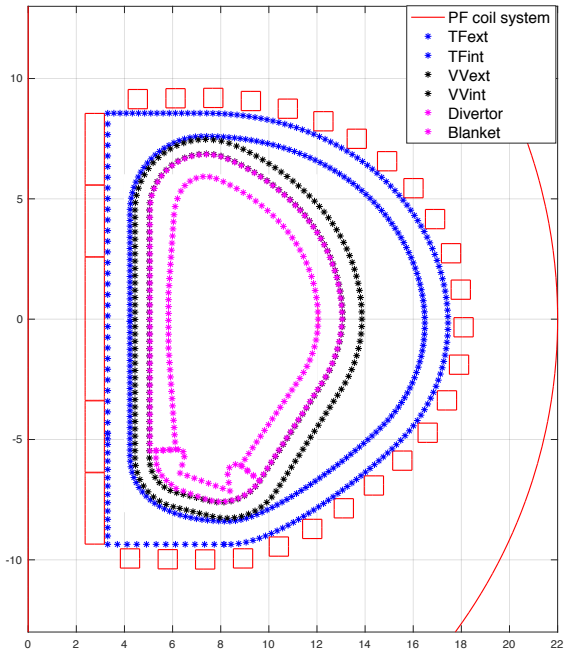

Figure 4. Redundant PF coils systems compatible with the 2017 DEMO device geometrical description

It is implemented in terms of a quadratic optimization problem with linear and quadratic constraints. Then, the shape and current optimization of the initial configuration can be achieved by solving the following LQ minimization problem.

The idea beneath the optimization procedure is the definition of a linearized model that relates the variation of the currents in the redundant CS/PF coil system $\delta I_{CS/PF}$ to the variation of the quantities related to the constraints listed in Section 3.1. Therefore, the analysis of the *i-th* candidate PF coil systems turns out into an optimization problem over the linearized model implemented on a selected subset of the redundant coils:

$$\min_{\delta I^i_{CS/PF}} \left(I^i_{eq} + \delta I^i_{CS/PF}\right)^T \left(I^i_{eq} + \delta I^i_{CS/PF}\right) \tag{11}$$

subject to

$$\left\| \boldsymbol{C_G S_i^T} \delta I^i_{CS/PF} \right\| < \Delta g \tag{12.1}$$

$$\left\| B^i_{eq} + \boldsymbol{C_{B_{pol}} S_i^T} \delta I^i_{CS/PF} \right\| < B^i_{max} \tag{12.2}$$

$$\left\| I^i_{eq} + \delta I^i_{CS/PF} \right\| < I^i_{max} \tag{12.3}$$

and the vertical force constraints (8)-(9)-(10) in Section 3.1, where

- $\boldsymbol{S_i} \in R^{n \times N_{CS/PF}}$ is a selection matrix picking the coils of the *i-th* candidate PF coil system among all the PF coils of the redundant system;
- $I^i_{eq} \in R^n$ is the vector of CS/PF currents in the coils of the *i-th* candidate PF coil system at the reference equilibrium evaluated as:

$$I^i_{eq} = \left(\boldsymbol{C_G S_i^T}\right)^{\dagger} \boldsymbol{C_G} I_{eq}$$

  with $I_{eq} \in R^{N_{CS/PF}}$ the vector of CS/PF currents in the redundant PF coil system at the reference equilibrium;

- $\delta I^i_{CS/PF}$ are the optimized CS/PF current variations in the coils of the *i-th* candidate PF coil system. The total optimized currents are $I^i_{opt} = I^i_{eq} + \delta I^i_{CS/PF}$;
- $B^i_{eq} \in R^n$ is the vector of the poloidal magnetic field in the coil locations of the *i-th* candidate PF coil system;
- Δg indicates the maximum acceptable variation of the gaps with respect to the reference configuration.

Note that the inequalities (12) can be easily converted into linear constraints with respect to the optimization variables $\delta I_{CS/PF}$ defining, with the quadratic objective function (11), a convex LQ optimization problem [17]-[18].
Concerning the vertical force constraints, it is possible to express the vector of the vertical forces on the PF coils of the *i-th* candidate PF coil systems as

$$F^i_{CS/PF} = \left(B^i_{eq} + \boldsymbol{C_{B_{pol}}} \boldsymbol{S_i^T} \delta I_{CS/PF}\right) \circ \left(I^i_{eq} + \delta I^i{}_{CS/PF}\right)$$

where $\circ$ indicates the Hadamard product. Therefore, the inequalities (8)-(10) define quadratic constraints that are not compatible with the LQ formulation and hence give rise to the definition of a non-convex optimization problem whose solution is strongly affected by the initial condition.

The proposed strategy for the definition of the optimized PF coil system is therefore divided in two steps. A preliminary optimization phase where the LQ optimization problem (11)-(12) is solved for all the candidates PF coil systems. This phase allows a drastic reduction of the cases among which the optimal PF coil system could be determined with a huge reduction of the computing time. A second phase where the non-convex quadratic optimization problem with quadratic constraints is then implemented on the remaining PF coils system candidates assuming as initial condition the solution of the LQ optimization problems.

Remark: It is important to recognize that the elongation, triangularity and grazing angle constraints have not been considered in the optimization problem taking into account that the reference equilibria has been designed to guarantee these constraints and the vector Δg is choosen enough small to maintain an almost fixed plasma separatrix.

4 An example of application

In this section, an application of the PF coils optimization procedure on DEMO fusion reactor is proposed. Indeed, the main parameters of the DEMO device are firstly presented; then a detailed description of the constraints is proposed and finally the results of the optimization procedure are shown.

4.1 DEMO geometrical description and reference plasma configuration

The design of a fusion device is usually performed using systems codes able to assess the engineering and economic viability of a hypothetical fusion power station using simple models of all parts of a reactor system. For DEMO device, the systems code PROCESS [19] is used to identify the relevant parameters assuming a net-electric power output of 500MW. In the present section, we apply the proposed PF coil optimization algorithm on the DEMO Single Null baseline 2017 whose main parameters defined by PROCESS [20] are reported in Table I.

Table I: Main parameters of DEMO baseline 2017 defined by PROCESS [20].

Geometrical parameters		
Major radius	R_0 (m)	8.938 m
Minor radius	a (m)	2.883 m
Aspect ratio	A	3.10
Elongation	k_{95}	1.65
Truangularity	$\delta_{95\%}$	0.33
Volume	V	2266 m^3
Magnetic field on axis	B_0	4.89 T
Plasma physic parameters		
Plasma current	Ip	$19.07MA$
Poloidal beta	β_{pol}	1.141
Internal inductance	l_i	0.8

Once the DEMO relevant parameters have been identified, a reference plasma shape is defined geometrically. Then, the geometry of the machine, i.e. first wall, divertor structure, vessel and TF coil shells, is designed; dimension and position of the components are then optimized taking into account their realistic realization, as shown in figure 4. Finally, the reference plasma scenario composed by the pre-magnetization, the start of flat top (SOF) and end of flat top (EOF) is designed assuming a non-optimized PF coil system, as shown in Figure 5. The dimension and position of the CS stack is fixed in accordance with to the maximum magnetic field constraint [PROCESS run]. The premagnetization flux is around $\Psi(t_{BD}) = 310Vs$; the flux at SOF is identified using the Ejima formula [16] while the flux at EOF is defined as minimum flux reachable at flat top maintaining an almost fixed plasma separatrix and it is mainly related to the capability of the CS stack.

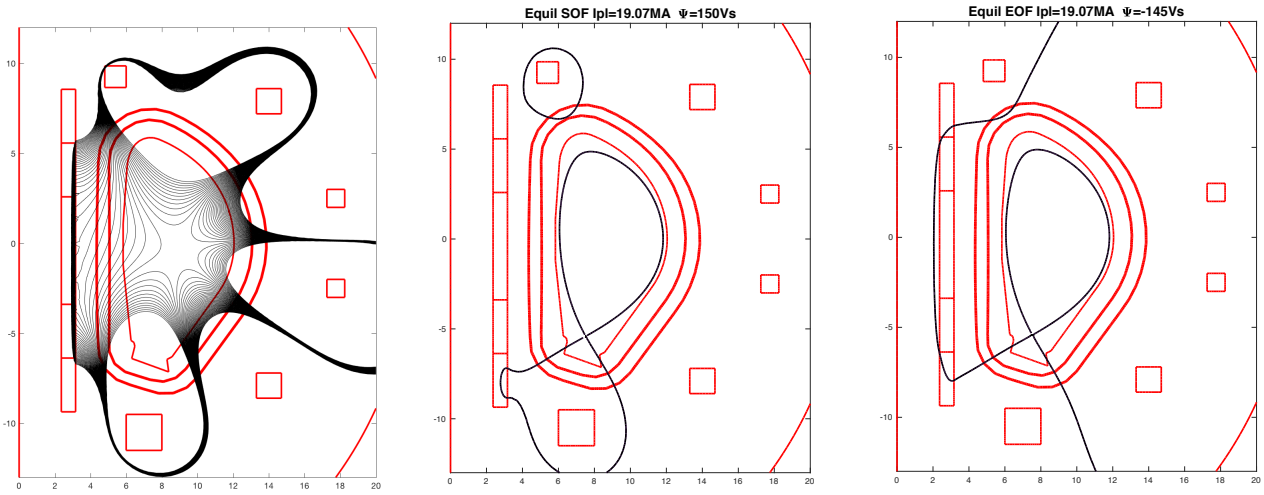

Figure 5. Plasma scenario at premagnetization, SOF and EOF.

4.2 Constraints definition in DEMO

PF coil currents

The current density limit in DEMO is $J_{max} = 12.5\ MA/m^2$ for all the CS/PF coils.
The dimension and position of the CS stack has been fixed accordingly to the maximum magnetic field constraint [PROCESS run], while the maximum area of the PF coils has been imposed equal to $4m^2$, corresponding to a maximum current in a single PF coil of $50\ MAturns$.

Magnetic field

The maximum magnetic field at the location of the PF and CS coils for a safe design of the conductors and the winding packs shall not exceed $12.5\ T$.

Vertical Forces on the PF/CS coils

DEMO vertical force constraints on the PF/CS coils are:

- maximum vertical force on a single PF shall not exceed 450 MN;
- maximum vertical force on the CS stack shall not exceed 300 MN;
- maximum separation force in the CS stack shall not exceed 350 MN.

Plasma Separatrix

The DEMO constraints on the plasma separatrix are

- the minimum plasma-wall distance should be $0.225\ m$;
- the minimum grazing angle should be 1.5°;
- reference plasma elongation at the 95% of the separatrix flux $k_{95\%} = 1.65$
- reference plasma triangularity at the 95% of the separatrix flux $\delta_{95\%} = 0.33$
- reference flat top flux swing around $300Vs$

4.3 Results of the optimization procedure in DEMO device

In order to define an optimized set of PF coils satisfying all the currents and vertical forces constraints, a redundant set of 30 coils (5 for the CS and 25 for the PF, respectively) compatible with the available space limited by the outer TF shell has been produced, as shown in Figure 6.

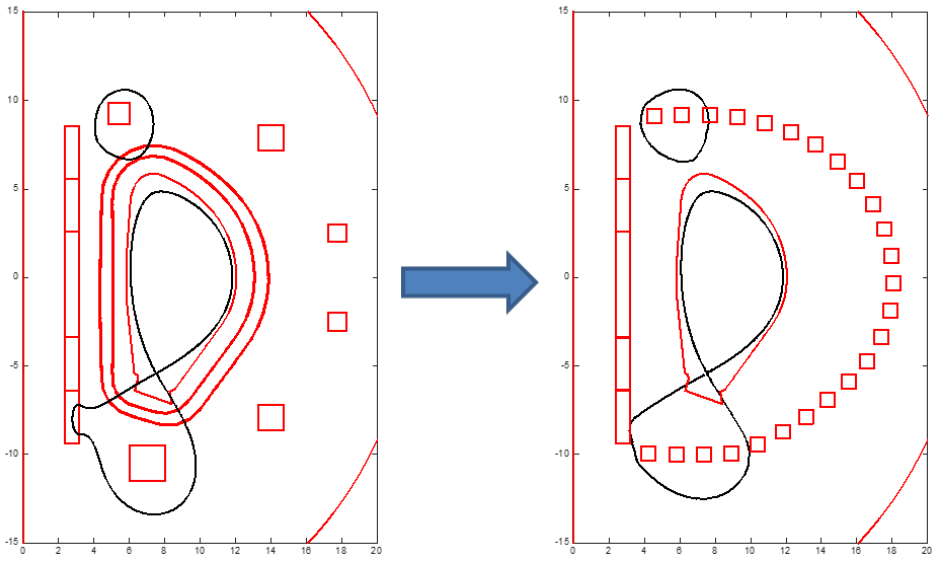

Figure 6. Redundant PF coil system for the 2017 SN baseline at flat-top

All the PF coils have the same cross-section of $0.64\ m^2$. The number of possible PF coil systems composed by 6 over 25 PF coils is given by $\binom{25}{6} = 177100$. However, this number has been reduced to 5005 considering a constraint on the minimum distance between the centers of the cross sections of adjacent coils center, i.e. $d \geq 3m$. In the present analysis, possible geometric constraints (e.g., port locations for diagnostics, additional heating and remote maintenance) are only considered in the post-processing of the solutions.

An exhaustive analysis of the 5005 candidate PF coil systems has been then carried out in order to find SOF and EOF configurations able to maximize the flat-top flux swing while maintaining the desired plasma shape within a certain tolerance and verifying all field and vertical force constraints summarized in Section 4.2. The exhaustive analysis has been performed using the CREATE-NL [9] equilibrium code and the CREATE-L [10] linearization code solving first an LQ minimization problem (11)-(12) in order to reduce the coil sets among which the optimal PF coil system could be determined. Finally the quadratic constraints (8)-(10) related to the force limits have been added.

Equilibrium and linearization evaluation with a course finite element triangular mesh of 13000 points required a CPU time of about 300s, whereas the full exhaustive analysis took additional 200s (to be repeated at SOF and EOF) on a MacBook Pro 2.5 GHz Intel Core i7.

Due to the high number of PF coils solutions able to guarantee all the constraints in Section 4.2, we focus our attention on the subset of PF coil systems limiting the vertical forces on the PF coils below 200 MN. Six possible solutions have been found and shown in Figure 7.

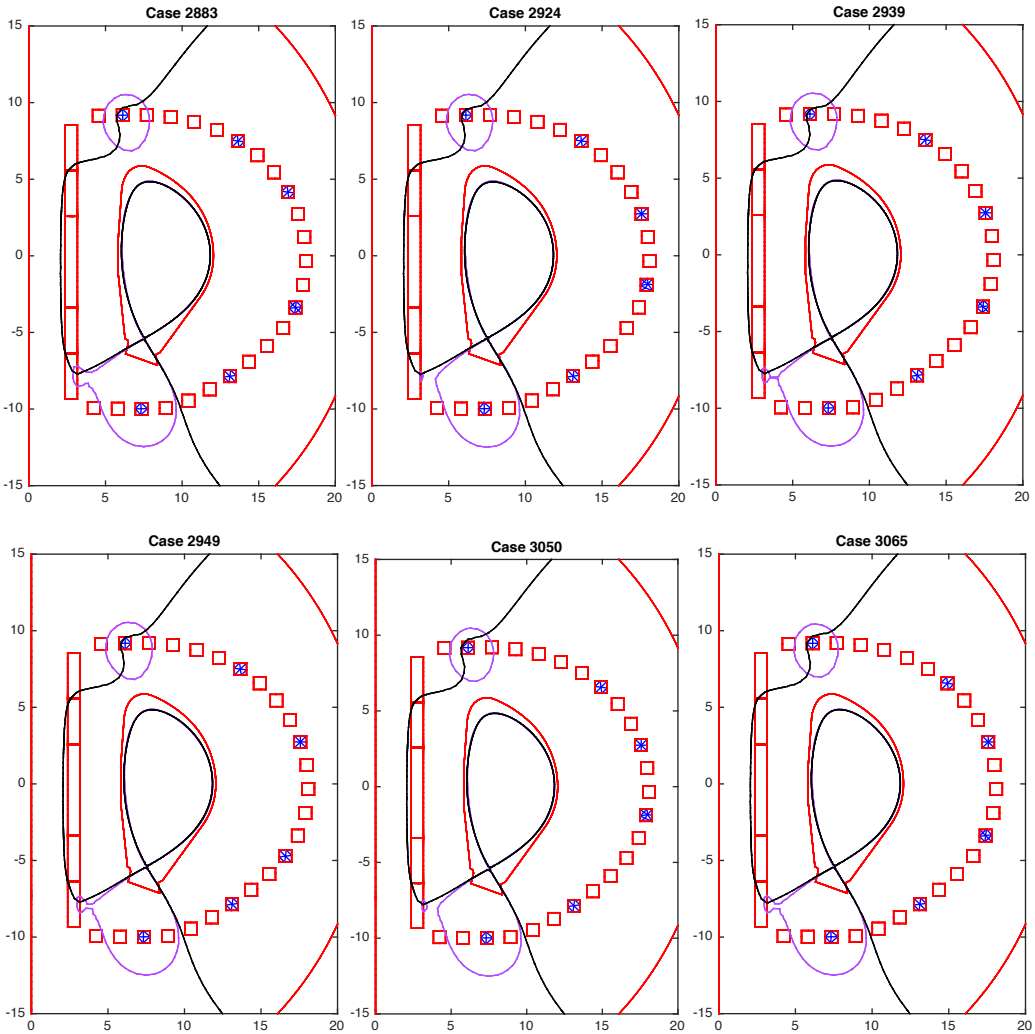

Figure 7. Candidate PF coil systems verifying the constraints in Section 3.2 with the maximum vertical force on a single PF coil below 200 MN.

Table II reports the main costs and constrained quantities of the selected PF coil systems.

Table II: Costs and constraints of the candidate PF coil systems

Costs \ PF coil system	**Flux swing at flat top (V·s)**	**$\Sigma\|I_{PF/CS}\|_{max}$ (MAturns)**	**Max PF coils current (MAturns)**	**Max. force on a single coil $F_{z,PF}$ (MN)**	**Max. vertical force on CS $F_{z,CS}^{total}$ (MN)**	**Max. CS separation force $F_{z,CS}^{sep}$ (MN)**
2883	298.27	179.74	14.95	149.26	131.47	131.47
2924	298.27	180.36	15.46	157.54	132.18	132.18
2939	298.27	180.14	15.23	151.12	128.04	128.04
2949	298.27	179.67	15.29	146.5	127.51	127.51
3050	298.25	179.99	15.56	151.04	134.73	134.73
3065	298.27	180.4	15.29	153.26	133.53	133.53

According with Table II, the six PF coil systems are almost equivalent. However, to allow the presence of an adequate equatorial access port, the final choice went to the solution "2883". For this configuration, a PF coil system with the 6 selected PF coils of appropriate dimensions has been produced. The set of PF coil currents defined by the optimization problem at SOF and EOF has been used to fix the dimension of the coils according to the current density constraint of $J_{max} = 12.5\ MA/m^2$. Moreover, a slight modification of the PF coil positions has been imposed to ensure a distance from the TF coil outer shell of $10\ cm$. Figure 8 shows the optimized PF coil system with the equilibria at SOF (magenta) and EOF (black) evaluated with the CREATE-NL equilibrium code.

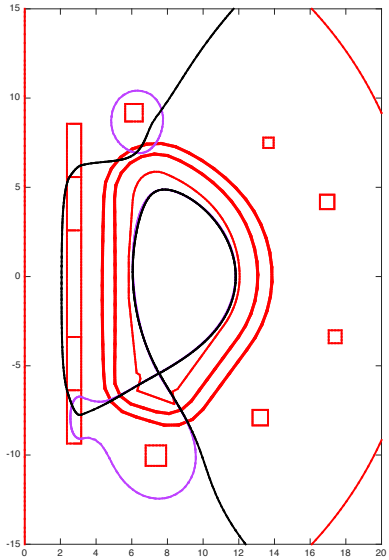

Figure 8. SOF (magenta) and EOF (black) Single Null optimized configurations

Table III reports the the main costs and constrained quantities.

Table III: Costs and constrained quantities of the candidate PF coil systems

Costs \ PF coil system	**Flux swing at flat top (V·s)**	**$\Sigma\lvert I_{PF/CS}\rvert_{max}$ (MAturns)**	**Max PF coils current density (MA/m^2)**	**Max. force on single coil $F_{z,PF}$ (MN)**	**Max. vertical force on CS $F_{z,CS}^{total}$ (MN)**	**Max. CS separation force $F_{z,CS}^{sep}$ (MN)**
original	295.72	182.68	12.49	181.14	145.63	145.63
"2883"	298.27	179.74	14.95	149.26	131.47	131.47
optimized	298.10	181.47	12.50	145.29	111.72	111.72

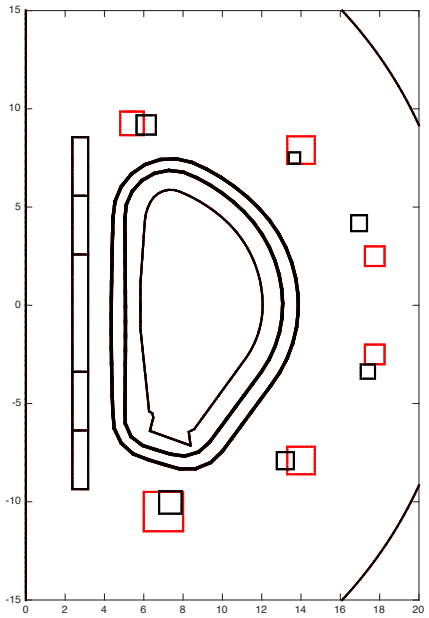

Figure 9. Original (red) and optimized (black) PF coil systems

Table III shows that the optimization of the PF coil systems does not affect the flux swing between SOF and EOF (it is mainly related to the CS coils) while a 20% improvement can be noted on the maximum vertical force on the CS and PF coils. Figure 9 and Table IV show a comparison between the original (see Figure 5) and the refined PF coil systems.

Table IV: Original and optimized PF coils system

	R [m]		**Z [m]**		**DR [m]**		**DZ [m]**		**AR [m^2]**	
	Init	**Opt**	**Init**	**Opt**	**Init**	**Opt**	**Init**	**Opt**	**Init**	**Opt**
P1	5.4	6.12	9.26	9.18	1.2	0.98	1.2	0.98	1.44	0.97
P2	14	13.66	7.9	7.50	1.4	0.58	1.4	0.58	1.96	0.34
P3	17.75	16.95	2.5	4.18	1	0.81	1	0.81	1	0.66
P4	17.75	17.41	-2.5	-3.37	1	0.72	1	0.72	1	0.52
P5	14	13.20	-7.9	-7.91	1.4	0.87	1.4	0.87	1.96	0.76
P6	7	7.35	-10.5	-10.03	2	1.15	2	1.15	4	1.32

5 Conclusions

In this paper, a new approach for the optimization of the PF coil system in axisymmetric fusion devices has been presented. The proposed procedure allows to optimize the number, position and dimension of the PF coils reducing, at the same time, currents and forces on the coils while fulfilling the machine technological constraints.
The efficiency of the procedure has been shown through an application to the DEMO reactor. In particular, for the Single Null baseline 2017 configuration, a reduction of around 20% on the maximum vertical force acting on the CS and PF coils has been obtained.
The present study arises from the need for a tool able to optimize the PF coil system reducing, at the same time, currents and forces on the coils. Since it is uncertain whether the conventional divertor solution, based on the single null magnetic configuration also adopted for ITER, will extrapolate to the considerably more severe exhaust requirements in DEMO [8][4], several non-conventional magnetic configurations (e.g. snowflake divertor, X divertor, double nulls) as well as liquid metal divertor targets are considered as alternatives. In this framework, a versatile tool fulfilling different aims, depending on plasma configuration, could be crucial. Indeed, although the plasma alternative configurations could constitute a reliable solution for the power exhaust issue, preliminary analyses on alternative configurations in a DEMO-like tokamak [21]-[22], revealed inherent difficulties in obtaining them with low coil currents and to handle the forces on the poloidal field (PF) and central solenoid (CS) coil system. In that sense, a flexible tool able to optimize number and position of the PF coils reducing the currents and the forces while fulfilling the machine technological constraints seems to be essential.

Acknowledgements

The authors gratefully thank Gianfranco Federici ,Francesco Maviglia and Holger Reimerdes for their useful suggestions. This activity was carried out under the EUROfusion Work Packages PMI on the definition of standard configurations for the DEMO device. This work has been carried out within the framework of the EUROfusion Consortium and has received funding from the Euratom research and training programme 2014-2018 under grant agreement No 633053. The views and opinions expressed herein do not necessarily reflect those of the European Commission.

References

[1] Lister, J. B., Portone, A., Gribov, Y.: Plasma control in ITER. IEEE Control Syst. Mag, 26, 79-91, (2006).
[2] Fusion Electricity – A roadmap to the realisation of fusion energy, November 2012 (http://users.euro-fusion.org/iterphysicswiki/images/9/9b/EFDA_Fusion_Roadmap_2M8JBG_v1_0.pdf)
[3] Federici, G., et al.: Overview of EU DEMO design and R&D activities. Fusion Engineering and Design, 89, 882-889, (2014).
[4] Ambrosino, R., Albanese, R., et al.: Optimization of experimental snowflake configurations on TCV. Nuclear Fusion, 54, (2014).
[5] H. Grad and H. Rubin, in Proceedings of 2nd UN Conference on the Peaceful Uses of Atomic Energy, Vol. 31, p. 190 (1958).
[6] V. Shafranov, Sov. Phys. JETP 6, 545 (1958).

[7] Albanese, R, Ambrosino, R., Mattei, M.: A procedure for the design of snowflake magnetic configurations in tokamaks. Plasma Physics and Controlled Fusion, 56, (2014).
[8] Albanese, R.: DTT: A divertor tokamak test facility for the study of the power exhaust issues in view of DEMO. Nuclear Fusion, 57, (2017).
[9] Albanese, R, Ambrosino, R., Mattei, M.: CREATE-NL+: A robust control-oriented free boundary dynamic plasma equilibrium solver. Fusion Engineering and Design, 96-97, 664-667, (2015).
[10] Albanese, R., Villone, F.: The linearized CREATE-L plasma response model for the control of current, position and shape in tokamaks. Nuclear Fusion, 38, (1998).
[11] Luxon, J. L., Brown, B. B.: Magnetic analysis of non-circular cross-section tokamaks. Nuclear Fusion, 22, 813, (1982).
[12] Albanese, R., Mattei, M., Calabrò, G., Villone, F.: Unified treatment of forward and inverse problems in the numerical simulation of tokamak plasmas", Int. Symp. Applied Electromagnetics and Mechanics (Versailles, 2003).
[13] Ambrosino, R., Albanese, R., Castaldo, A., Loschiavo, V. P., McIntosh, S., Reimerdes, H.: WPDTT1 Final Report 2016 on Activity DTT1-AC3: Equilibrium generation. https://idm.euro-fusion.org/?uid=2MV7L9.
[14] Matthews, G. F., et al.: Investigation of the fluxes to a surface at grazing angles of incidence in the tokamak boundary. Plasma Physics and Controlled Fusion, 32, 1301-1320 (1990).
[15] Huber, A., et al.: Comparative H-mode density limit studies in JET and AUG. Nuclear Materials and Energy, 12, 100-110 (2017).
[16] Ejima, S., et al.: Volt-second analysis and consumption in Doublet III plasmas. Nuclear Fusion, 22, 1313 (1982).
[17] Potra, F. A., Wright, S.J.: Interior-point methods. Journal of Computational and Applied Mathematics, 124, 281-302 (2000).
[18] Coleman, T. F., Li, Y.: A Reflective Newton Method for Minimizing a Quadratic Function Subject to Bounds on Some of the Variables. SIAM J. Optim., 6 (4), 1040-1058 (1995).
[19] Kovari, M., et al.: "PROCESS": A systems code for fusion power plants—Part 2: Engineering. Fusion Engineering and Design, 104, 9-20 (2016).
[20] Kovari, M.: PROCESS runs for new baseline design EU DEMO1 2017: 02.05.2017.
[21] Asakura, N., et.al, Trans. Fus. Sci. Tech. 63 (2013) 7.
[22] Albanese, R., Ambrosino, R., Mattei, M.: WPPMI Final Report 2014 on Deliverable: Vertical Stability. https://idm.euro-fusion.org/?uid=2L7CZV.